ISSN 0010-5082, Combustion, Explosion, and Shock Waves, 2019, Vol. 55, No. 2, pp. 156–166. © Pleiades Publishing, Ltd., 2019.
Original Russian Text © K.O. Sabdenov, M. Erzada.

Simulation of Combustion of Solid High-Energy Materials with Account for Erosive Effects

K. O. Sabdenov[a] **and M. Erzada**[a]

UDC 536.46

Published in *Fizika Goreniya i Vzryva*, Vol. 55, No. 2, pp. 38–49, March–April, 2019.
Original article submitted January 1, 2018; revision submitted May 23, 2018; accepted for publication May 23, 2018.

Abstract: A negative erosive effect arises in the simulation of combustion due to a generated turbulent motion in the gasification zone of a solid energy material. A thermal energy in the gasification zone comprises the heat of chemical sources in it and the heat coming up to the gasification surface from the flame zone in a gaseous phase. Some of this energy returns to the gaseous phase in the form of the mechanical energy of turbulent motion, and this turbulence cools down the gasification zone. This model is used to explain the weakening of the negative erosive effect, observed in the experiments, with increasing pressure and decreasing initial temperature.

Keywords: gasification surface, internal turbulence, erosion factor, Vilyunov–Dvoryashin effect.

DOI: 10.1134/S0010508219020047

INTRODUCTION

The motion of gaseous products of combustion along the gasification surface of a solid energy material (blowing) changes the burning rate. This is determined by an erosion factor during combustion $\varepsilon = u_w/u_0$, where u_w and u_0 are burning rates for blowing velocities $w \neq 0$ and $w = 0$. If the burning rate rises, then this is a positive erosive effect discovered by Leipunskii in 1930s [1] (the Leipunskii effect). Leipunskii also notes the threshold nature of this phenomenon: the erosion factor increases after the blowing velocity w exceeds some threshold value w_*. The top limit $\varepsilon_{\max}$ is not established yet. The nature of the velocity threshold w_* and approximate theoretical approach to calculating it are described in [2].

The decrease in the burning rate discovered later [3, 4] is known as a negative erosive effect (the Vilyunov–Dvoryashin effect). The burning rate drops during blowing of the gasification surface in tests with homogeneous [3, 4] and heterogeneous [5, 6] propellants. Therefore, the Vilyunov–Dvoryashin effect is explained on the basis of general physical processes, where the particular composition of an energy material is simply a secondary factor.

[a]North Kazakhstan State University named after M. Kozybayev, Petropavlovsk, 150000 Kazakhstan; sabdenovko@yandex.kz.

1. BRIEF REVIEW OF THE MODERN STATE OF THE THEORY OF A NEGATIVE EROSIVE EFFECT

In theoretical studies [7–10], an erosion factor cannot be smaller than a theoretically minimal value $\varepsilon_{\min} = 1/\sqrt{e} \approx 0.61$. If $\varepsilon < \varepsilon_{\min}$, then combustion is unstable and can fail. Instability is also possible with $\varepsilon > \varepsilon_{\min}$, which is dependent on the closeness of combustion parameters to the stability boundary determined by a large number of other physical parameters. Until the present moment, the smallest observed value of an erosion factor in tests is 0.7–0.73 [5, 6]. The Vilyunov–Dvoryashin effect is observed in the case of relatively low blowing velocities w. A further increase in w makes ε larger due to a turbulent flame in the gaseous phase, which stimulates the development of a positive erosive effect [7].

It is noted in [7–10] that the Vilyunov–Dvoryashin effect may manifest in semiclosed spaces [3–6], in which case some of the inner energy of combustion products transforms into a mechanical (kinetic) energy of motion along the propellant surface, and, as a result, an erosive effect is observed. If blowing in the experiments comes from a stream of a hot gas and there is no mechanical work [11–13], then the erosive effect is positive only.

In the experiments, a blowing stream has a characteristic velocity $w_\infty = \text{const}$ (w_∞ is the gas velocity on the axis of a cylindrical combustion chamber in rocket engines). More universal dependences of the erosion factor can be determined using the Vilyunov number Vi or the Bulgakov–Lipanov number Θ [7, 9]:

$$\text{Vi} = \sqrt{\zeta}\,\frac{\rho w_\infty}{\rho_c u}, \quad \Theta = \frac{\delta_b}{\delta_g}.$$

Here ζ is the drag coefficient, ρ and ρ_c are the densities of gas and condensed phase of the propellant, δ_b is the thickness of the combustion zone in the gaseous phase, and δ_g is the thickness of the viscous sublayer in the turbulent boundary layer. The Vilyunov number can be conveniently used to process and represent experimental data [11, 12], and the Bulgakov–Lipanov number is more suitable for theoretical studies [7, 9]. The requirement for the Leipunskii effect to work is that $\Theta > 1$. If $\Theta < 1$, the Vilyunov–Dvoryashin effect may be observed [2, 7, 9]. In theory [2, 7–10], there are two blowing velocity scales:

$$w_0 = \sqrt{c_p T_b}, \quad w_* = \frac{32.5}{\sqrt{\zeta}}\,\frac{\nu}{\delta_b}.$$

Here c_p is the heat capacity of gaseous products of combustion at constant pressure, T_b is the flame temperature in the gas or combustion temperature, and ν is the kinematic viscosity of the gas. Typical scale velocities are $w_0 \approx 10^3$ and $w_* \approx 10^2$ m/s. The primer characterizes the Vilyunov–Dvoryashin effect, and the latter describes the Leipunskii effect. According to the theory of similarity and dimensionality [14], the erosion factor ε can be represented as a function of two dimensionless parameters V_1 and V_2:

$$\varepsilon = F(V_1, V_2) = F\left(\frac{w_\infty}{w_0}, \frac{w_\infty}{w_*}\right),$$

$$V_1 = \frac{w_\infty}{w_0}, \quad V_2 = \frac{w_\infty}{w_*}.$$

Further in the positive direction of the w_∞ coordinate, a negative erosive effect is observed initially, and then the first threshold blowing velocity w_{*1} is exceeded ($w_\infty > w_{*1}$), which increases the burning rate, while $\varepsilon < 1$. The velocity w_{*1} is the root of the equation $\dfrac{dF}{dw_\infty} = 0$. Next, as the second threshold velocity is reached $w_\infty = w_{*2}$, the erosion factor equals $\varepsilon = F = 1$, after which the burning rate can only become larger. As a rule, $w_{*1} \neq w_{*2}$, but there is no Vilyunov–Dvoryashin effect as long as $w_{*1} = w_{*2}$. An inverse process has never been observed in the experiments, i.e., a negative erosive effect never follows a positive erosive effect. This one-sided nature of the erosive effect and the existence of blowing velocities w_{*1} and w_{*2} can be explained as follows [7]: the Vilyunov–Dvoryashin effect manifests if the chemical reaction zone in the gaseous phase is located in the viscous sublayer, which means that combustion in the gaseous phase is predominantly laminar. As the blowing velocity becomes larger, the thickness of the viscous sublayer decreases, while the thickness of the combustion zone remains virtually constant. The relationship $w_\infty \approx w_{*1}$ determines the conditional boundary of transition of the laminar flame in the gaseous phase into a turbulent regime.

The burning rate of many solid energy materials u is exponentially dependent on temperature (pyrolysis law). In the absence of blowing, the temperature of the gasification surface is T_s and $u \sim \exp(-E_c/2RT_s)$, where R is the universal gaseous constant, and E_c is the activation energy of the bulk reaction of pyrolysis. The motion of combustion products along the gasification surface changes the balance of thermal energy in the whole combustion zone, and then the temperature of the gasification surface takes the value of $T_{s,w}$ and the burning rate $u \sim \exp(-E_c/2RT_{s,w})$. As the characteristic value of the activation energy of the chemical reaction is taken as $E_c \approx 8 \cdot 10^4$ J/mol and the temperature of the gasification surface is $T_s \approx 650$ K [15, 16], the smallest value $\varepsilon = \varepsilon_{\min} = 0.61$ corresponds to the maximal relative change of the temperature

$$\Delta_T = \frac{T_s - T_{s,w}}{T_{s,w}} = \frac{RT_s}{E_c} = 0.068.$$

Hence, it is necessary to determine the temperature of the gasification zone $T_{s,w}$ with a relative error not exceeding 1% and an absolute error $\Delta T_{s,w} \approx 44$ K. It is quite difficult to experimentally determine $T_{s,w}$ by the existing measurement means because of the small gasification thickness: ≈2–2.5 μm [15, 16]. Therefore, the validation of different theories of a negative erosive effect [7, 8, 17–25] is currently possible only on the basis of indirect data. Along with that, one should maintain a high accuracy of results of theoretical calculations, including the correct numerical solution of the equations of mathematical models.

The small value $\Delta_T \ll 1$ (or the value of $\Delta T_{s,w}$ is about several degrees) provides large opportunities for constructing the Vilyunov–Dvoryashin effect models, and the reasons for such an insignificant decrease in the temperature in the gasification zone can be quite many. However, there is at least one key experimental fact [4], which is the gradual extinction of the Vilyunov–Dvoryashin effect with the falling initial temperature of the propellant T_0. In theoretical studies [17–20,

22–25], this result is often ignored.* Any model of a negative erosive effect should probably be tested for predicting the key experimental fact [17, 21]. The fact that the Vilyunov–Dvoryashin effect weakens at high pressures [6] (propellant is a ammonium perchlorate/polyurethane) can also be interpreted as a more important experimental fact. But there are also other issues: how universal the vanishing of the Vilyunov–Dvoryashin effect at a low initial temperature and high pressure is and whether the decreasing burning rate during blowing should be equalized with the Vilyunov–Dvoryashin effect. It is known [6, 15] that the burning rate slightly drops in the case of acoustic instability. In this case, the blowing of the gasification surface is mainly due to acoustic oscillations of the gaseous products of combustion.

The manifestation of an erosive effect in mixed propellants and its relation to motions of gas similar to acoustic oscillations are described in [22–25]: a dimensionless vector of gas velocity near the gasification surface has longitudinal $\bar{w}$ and normal $\bar{v}$ components with amplitude A and wavelength λ_w:

$$\bar{w} = Ax\sin(\Omega t)\sin\left(\frac{2\pi y}{\lambda_w}\right),$$
$$\bar{v} = 1 - \frac{\pi A}{\lambda_w}x^2\sin(\Omega t)\cos\left(\frac{2\pi y}{\lambda_w}\right). \qquad (1)$$

Here the y coordinate is directed along the tangent, and the x coordinate is directed along the normal to the gasification surface, t is time, and Ω is the frequency. This choice of velocities is motivated by a difference in the gasification rates of components of the heterogeneous propellant, and these components are contained in the propellant as microscopic particles with an average size $a \approx 1$ μm. It can be approximately assumed that $\lambda_w \approx a$, so the spatial heterogeneity along with a difference in the gasification rates leads to the spatial and time heterogeneity of the vector of the velocity with which gaseous products flow out. Equations (1) quite roughly represent the real distribution of velocities w and v, there should be a small-scale turbulent motion of gas near the gasification zone of the heterogeneous propellant [27], and this motion is referred to as "internal turbulence" below.

The combustion of a mixed propellant with a more accurate approximation for a gas velocity vector is described in [23–25], where Eq. (1) is replaced by a wide range of velocities with different wavelengths and frequencies. This approach imitates internal turbulence very well. The main result of [23–25] is relationship $\varepsilon(A)$, and it is quite possible that $\varepsilon(A) < 1$ under certain conditions superimposed upon the chemical reaction rate in the solid phase. The reason for the Vilyunov–Dvoryashin effect is the formation of discontinuities in the flame front in the gas, with no combustion in the discontinuity regions. As a result, the heat flux to the gasification decreases along with the burning rate. The formation of a discontinuity can be explained as follows: the existence of a steady combustion front (flame) requires that diffusive, thermal, and hydrodynamic processes are concurrent. If the gas velocity v is larger than the normal velocity of the flame in the gas, then the gas flow entrains the combustion zone. If this excess of the velocity is local, then the plane front of the flame is deformed. The Markstein mechanism [28] can partially stabilize the flame front by the dependence of the flame velocity on the front curvature. However, if the local velocity of gas is high, the flame breaks, and this mechanism stops working.

There is another possible reason for the dropping burning rate [2]. As combustion products move along the gasification surface of the propellant, the momentum of the gas flow on a solid surface is lost [29]. Thus, there is an excess gas velocity in a negative direction relative to the motion of the flame. If turbulent transfer coefficients are small, then the flame in the gaseous phase should be moved away from the gasification surface, which then reduces the heat flux to this surface and the burning rate. The concept of small-scale turbulence also propagates in [22–25] on the case of the combustion of a homogeneous propellant. There is no doubt that a new mechanism of a negative erosive effect is discovered in these studies, but this mechanism is quite weak because the erosion factor in this model is $\varepsilon = 0.95$–1 [22–25]. However, it is important to substantiate the assumption that the theoretical results obtained correspond to the experimental data of Vilyunov and Dvoryashin [3, 4]. The observed phenomena are explained by the influence of large gas velocity gradients $\dfrac{\partial w}{\partial x}$ on combustion. This effect is mathematically strictly investigated in [30], with the results widely applied in the theory of turbulent combustion of gas mixtures [31]. The rough estimate of the gas velocity gradient that makes the manifestation of the Vilyunov–Dvoryashin effect possible is given in [7], and it is approximately 10^4 s^{-1}. This value is in good agreement with the results from [22–25].

Another explanation of the Vilyunov–Dvoryashin effect on the basis of internal turbulence near the gasification zone is given in [21], where the formation of chaotic motion is assumed to be the result of ther-

*The study of the dependence between the erosion factor ε and initial temperature T_0 in the model [20] is described in [26]. Apparently, ε either is totally independent of T_0 or decreases along with it, i.e., contradicts the experimental data [4].

mal instability. The reason for this instability is an excess heat release in the subsurface zone of gasification [16, 21]. Jackson's model, his group's model, and the Gusachenko–Zarko model rely on the hypothesis that there is a small-scale turbulence near the gasification zone, but are essentially different in how its effect on the burning rate is explained. In the Gusachenko–Zarko model, the blowing should suppress the internal turbulence and reduce the effective coefficient of thermal conductivity in the gaseous phase and heat flux to the gasification surface. This strictly contradicts the established physical picture of Jackson and others, where the blowing should improve the internal turbulence. This difference arises from a different nature of turbulence in these two models.

Small-scale turbulence near the gasification zone can be observed as a result of hydrodynamic instability [32], which is very similar to the Landau–Darrieus instability [28, 33]. The predicted hydrodynamic instability [32] is so strong that it cannot be fully suppressed by viscous forces and inertial effects [34]. Here perturbations with an arbitrary wavelength are localized in a relatively small vicinity of the gasification zone.

In a combustion model [35, 36], the turbulence in the gasification zone is developed by fracturing microscopic bubbles of gaseous products of decomposition of the solid phase. The formation of a mechanical turbulent motion uses the inner energy of the double-phase medium, and this can reduce temperature in the gasification zone or cause the Vilyunov–Dvoryashin effect. Turbulent motion is carried away by the gas stream into the flame zone, which means that the thermal energy is returned by the gasification zone into the gaseous phase in a mechanical form. Below the study is carried out on the basis of the model from [35, 36].

2. EQUATION FOR SIMULATING EROSIVE EFFECTS

This section is devoted to internal turbulence arising in the collapse of gas bubbles in the double-phase zone of gasification [36]. This small-scale turbulence is interesting for its high intensity and conversion of the larger part of the inner energy of the medium into the energy of mechanical motion of gas. The double-phase gasification zone is illustrated in Fig. 1. As the motion of gas is turbulent, here and below w and v are the average velocities of gas, which is not similar to Eq. (1).

If there is an exothermal chemical reaction with thermal effect Q_s in the gasification zone, then the real heat released Q_s' is smaller than Q_s [36]:

$$Q_s' = Q_s - e_{k,s}. \tag{2}$$

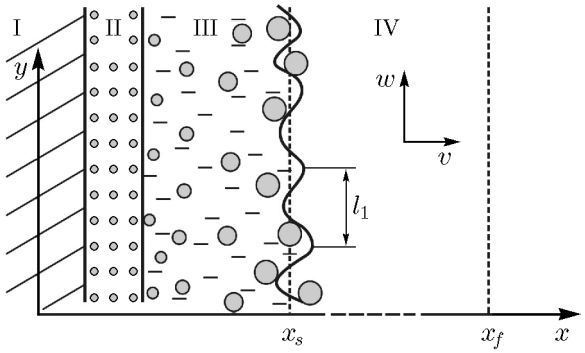

Fig. 1. Gasification zone: I is the solid phase, II is the zone where gas nuclei are formed in the solid phase, III is the liquid phase with gas bubbles, and IV is the gaseous phase; x_s and x_f denote the coordinates of the gasification surface and chemical reaction zone.

Here $e_{k,s}$ is the specific kinetic energy of turbulent motion, which is equal to the work performed by the gasification zone for forming this motion. The chaotic collapse of bubbles of diameter d_b and gas density ρ_s in the gasification zone creates turbulent motion with characteristic pulsations of the gas velocity v' and scale l_t [36]:

$$v' \approx \sqrt{\frac{\sigma_s}{\rho_s d_b}}, \quad l_t \approx d_b.$$

Here σ_s is the surface tension coefficient. This expression can be applied for bubbles whose diameters reach values up to $d_b \approx 10^{-8}$ m, while the effect of viscous forces should be taken into account in the case of smaller diameters for estimating v' [36]. The motion of gaseous products of combustion along the gasification surface with the characteristic velocity w_∞ should improve turbulence. On the one hand, this increases the coefficients of transfer and heat flux from the flame in the gas to the propellant surface. On the other hand, the conversion of heat into the kinetic energy of turbulent motion increases too. This energy is carried away with velocity v back into the flame zone, thereby creating a special thermal insulation of the gasification surface [35]. The dependence of turbulent pulsations of the gas velocity v' can be estimated using the approximate expression [35]

$$v'^2 = \frac{2\Delta p_*}{\rho_s} + b_1 w_\infty^2,$$

where Δp_* is the characteristic difference in pressures inside and outside the bubble, and b_1 is the constant. As v'^2 and $e_{k,s}$ differ in a factor of the order of unity and

$$v' \approx \sqrt{\frac{\sigma_s}{\rho_s d_b}}$$

in the case $w_\infty^2 = 0$, the following equation can be written:

$$e_{k,s} = \frac{3}{2}\frac{\sigma_s}{\rho_s d_b} + b_1 w_\infty^2. \quad (3)$$

Next, turbulence in the gaseous phase is under consideration. Here the determination of turbulent transfer coefficients is a complex and unsolved problem. Below these coefficients are generally denoted by D_t and the simplest representations in the form

$$D_t = \frac{1}{3} l_t v' + s^2 \frac{\partial w}{\partial x}, \quad (4)$$

where l_t is the turbulence length scale, s is the Prandtl mixing length, and the numerical factor 1/3 is introduced in analogy with molecular diffusion. The first term in Eq. (4) describes the transfer by internal turbulence, and the second one by the external turbulence arising in the motion of gaseous products of combustion along the propellant surface. The intensity of internal turbulence is the largest near the gasification surface $x_s(t)$, and it gradually drops under the influence of the forces of friction as the distance from it becomes longer.

In the region outside of the gasification zone, which is occupied by turbulent motion, the energy dissipates. The evolution of this motion is simulated using a small number of variables as the main ones, which are the specific kinetic energy e_k, dissipation rate ε, the characteristic value of turbulent pulsations of the velocity v', and linear scale l_t. Kolmogorov's theory of locally isotropic turbulence relates e_k, ε, and l_t [37]:

$$\varepsilon = a_1 \frac{e_k^{3/2}}{l_t}$$

(a_1 is the numerical factor). If there are no turbulence sources and diffusion energy transfer is weak in the gaseous phase, then changes in the kinetic energy can be written in the form of the differential equation

$$\frac{\partial e_k}{\partial t} + v\frac{\partial e_k}{\partial x} = -a_1 \frac{e_k^{3/2}}{l_t}, \quad (5)$$

where v is the average gas velocity in the direction of the x coordinate. Another equation is needed to determine all the turbulence parameters, and it is obtained from the condition of retaining of the square of total momentum of the pulse and the assumption of limitedness of the Loitsyansky integral [37, 38]:

$$l_t^5 e_k = a_2 = \text{const}. \quad (6)$$

Here a_2 can be obtained from the conditions of generation of turbulence in the gasification zone: $a_2 = e_{k,s} d_b^5$. The characteristic velocity of turbulent pulsations of the gas velocity v' are calculated from the equality [37, 39]

$$e_k = \frac{3}{2} v'^2, \quad (7)$$

where the factor 3/2 is introduced in analogy with molecular chaos in statistical physics.

Many solid propellants in the gasification zone contain a vaporizing liquid phase, and the chemical reaction of pyrolysis is occurring simultaneously in this zone (Belyaev–Zel'dovich model [16]). The gasification zone is very narrow, and the detailed investigation of all processes therein leads to complex mathematical equations. Therefore, the gasification zone is assumed to be the surface of discontinuity of the derivatives of temperature and relative concentration of the reacting substances in the brutto reaction A $\to$ B (see Fig. 1) with an effective activation energy E_c. This surface has the $x_s(t)$ coordinate and moves from the right to the left. In the region $x < x_s(t)$, there is a solid phase (substance A) with temperature T_c, density ρ_c, specific heat capacity c_c, and thermal conductivity λ_c. The region $x > x_s(t)$ is occupied by gas with temperature T, molar mass M_m, density ρ, pressure p, heat capacity at constant pressure c_p, and molecular thermal conductivity λ. In the region $x > x_s(t)$, the gasification products (substance B) are characterized by the relative concentration Y ($Y < 1$) and molecular diffusion coefficient D. Here only one chemical reaction occurs: B $\to$ C (C denotes the combustion products) with activation energy E.

In the model of combustion of solid high-energy material used below, the gasification zone (zone III in Fig. 1) is represented as a surface. Internal turbulence is generated only on this surface, and there is no interaction with external turbulence, which arises in the motion of gaseous products of combustion with velocity w. Such simplifying approximations make it possible to use Eqs. (2)–(7). Moreover, the small difference in the heat capacities of solid and gaseous phases can be ignored: $c_c = c_p$. Changes in the molecular mass of the reaction products and heat capacity c_p are ignored: $R_g = \text{const}$ and $c_p = \text{const}$. The subscript w of the temperature is omitted for simplicity. The mathematical form of the model is represented by the following equations:

for $-\infty < x < x_s(t)$,

$$\rho_c c_c \frac{\partial T_c}{\partial t} = \frac{\partial}{\partial x}\left(\lambda_c \frac{\partial T_c}{\partial x}\right); \quad (8)$$

for $x_s(t) < x < +\infty$,

$$\rho c_p \left(\frac{\partial T}{\partial t} + v\frac{\partial T}{\partial x}\right) = \frac{\partial}{\partial x}\left[(\lambda + \lambda_t)\frac{\partial T}{\partial x}\right] + \rho Q W + W_{g,s},$$

$$W_{g,s} = -\frac{\rho}{2}\left(\frac{\partial w^2}{\partial t} + v\frac{\partial w^2}{\partial x}\right) + \rho a_1 \frac{e_k^{3/2}}{l_t},$$

$$W = Yk_0 \exp\left(-\frac{E}{RT}\right), \quad l_t = d_b\left(\frac{e_{k,s}}{e_k}\right)^{1/5},$$

$$\rho\left(\frac{\partial Y}{\partial t} + v\frac{\partial Y}{\partial x}\right) = \frac{\partial}{\partial x}\left[(D + D_t)\rho\frac{\partial Y}{\partial x}\right] - \rho W,$$

$$\frac{\partial e_k}{\partial t} + v\frac{\partial e_k}{\partial x} = -a_1\frac{e_k^{3/2}}{l_t},$$

$$\frac{\partial \rho}{\partial t} + \frac{\partial}{\partial x}\rho v = 0, \quad p = \rho R_g T.$$

Boundary conditions are:

for $x \to -\infty$, $\quad T_c = T_0$;

for $x = x_s(t)$, $\quad -\rho_c\frac{dx_s}{dt} = -\rho\frac{dx_s}{dt} + \rho v, \quad e_k = e_{k,s},$

$$-\rho_c\frac{dx_s}{dt} = -\rho\frac{dx_s}{dt} + \rho v Y - (D + D_t)\rho\frac{\partial Y}{\partial x},$$

$$-\rho_c\frac{dx_s}{dt} = m(T_s, p),$$

$$T_s = T_c(t, x_s(t)),$$

$$\lambda_c\frac{\partial T_c}{\partial x} = (\lambda + \lambda_t)\frac{\partial T}{\partial x} - Q'_s\rho_c\frac{dx_s}{dt},$$

$$T = T_c;$$

for $x \to +\infty$, $\quad \frac{\partial T}{\partial x} = 0, \quad \frac{\partial Y}{\partial x} = 0.$

Here k_0 is the factor in front of the exponent in the Arrhenius law, R_g is the gaseous constant, $R_g = R/M_m$, λ_t is the coefficient of turbulent thermal conductivity of gas, $m(T_s)$ is the mass burning rate, and T_s is the temperature on the gasification surface. The kinetic energy of turbulence in the gasification zone $e_{k,s}$ is determined by Eq. (3). The initial conditions for system (8) are taken as their stationary solutions in the limit of an infinitely thin zone of chemical reactions in the gaseous phase ($E \to \infty$). These solutions in dimensionless form are given in [10].

For the propellant gasification rate u, the simple equation can be written [6, 15, 40, 41]:

$$u = -\frac{dx_s}{dt} = u_* \exp\left(-\frac{E_c}{2RT_s}\right), \quad u_* = \text{const}.$$

This makes it possible to determine the mass gasification rate $m(T_s) = \rho_c u$. The dependences of the molecular diffusion coefficients D, thermal conductivity λ and viscosity ν of gas on pressure p and temperature T are taken in the form [10]

$$D = D_0\frac{p_0}{p}\left(\frac{T}{T_0}\right)^2, \quad \lambda = \lambda_0\frac{T}{T_0},$$

$$\nu = \nu_0\frac{p_0}{p}\left(\frac{T}{T_0}\right)^2,$$

where D_0, λ_0, and ν_0 are the values of D, λ, and ν in the case where $T_0 = 293$ K and $p_0 = 10^5$ Pa. The scale v_* contained in the determination of the dimensionless velocity ω can be calculated using the expression $v_* \approx 0.045 w_\infty$ [10, 29].

The purpose of this study is to search for steady solutions of Eqs. (8) by the relaxation method, so the following equalities are taken for simplicity:

$$\frac{\partial e_k}{\partial t} = 0, \quad \frac{\partial \omega}{\partial t} = 0.$$

The mixing length s and the components y of the gas velocity vector w are determined using the equations [42]:

$$s\frac{d^2 s}{dx^2} - \frac{1}{2}\left(\frac{ds}{dx}\right)^2 - \frac{\gamma}{\nu}s^2\frac{dw}{dx}\left(1 - \frac{1}{\mu}\frac{ds}{dx}\right) = 0, \quad (9)$$

$$\nu\frac{dw}{dx} + s^2\left(\frac{dw}{dx}\right)^2 = v_*^2, \quad \gamma = 0.15, \quad \mu = 0.395.$$

The equations of the turbulent boundary layer should be solved under the conditions [42]:

for $x = x_s(t)$,

$$\frac{d^2 s}{dx^2} = q\frac{v_*}{\nu}, \quad q = 4.23 \cdot 10^{-3}; \quad s = 0; \quad w = 0.$$

3. SIMULATION RESULTS

The guiding physical idea of this study is as follows: the combustion of solid high-energy materials is always accompanied by turbulence and its source is a gasification zone. If there is motion of gaseous products of combustion along the gasification surface, then there is also external turbulence. Gas moves in a semiclosed space, so some of its inner energy is converted into a kinetic energy. All these factors actively affect the combustion process: internal turbulence and energy conversion always reduce the burning rate, and external turbulence increases the burning rate. On the basis of this model, the joint influence of two given types of turbulence on the burning rate should be analyzed.

The numerical solution of equations in system (8) is carried out by an implicit conservative scheme [43]. Approximation errors for Eqs. (8) and (9) have the order of $(\Delta x)^2$ in a spatial step $\Delta x = 10^{-6}$ m, and the time accuracy of the first order in the step $\Delta t = 10^{-6}$ s [the Courant dimensionless number is $\varkappa_c \Delta t(\Delta x)^{-2} \approx 0.43$].

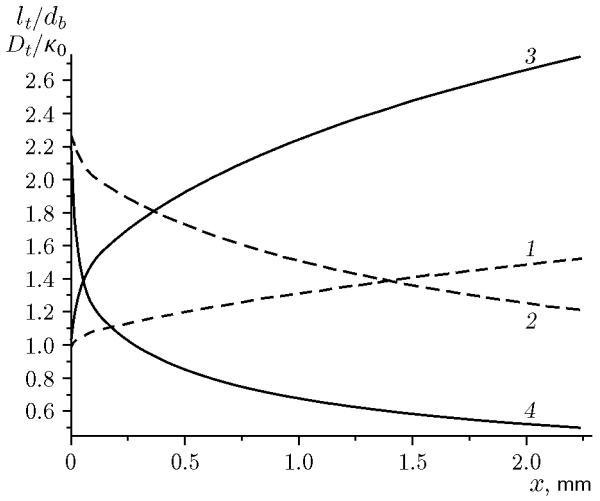

Fig. 2. Scale l_t/d_b (curves *1* and *3*) and the dimensionless coefficient of turbulent diffusion $D_t/\varkappa_0$ (curves *2* and *4*) versus the x coordinate for $a_1 = 10^{-8}$ (*1* and *2*) and 10^{-7} (*3* and *4*).

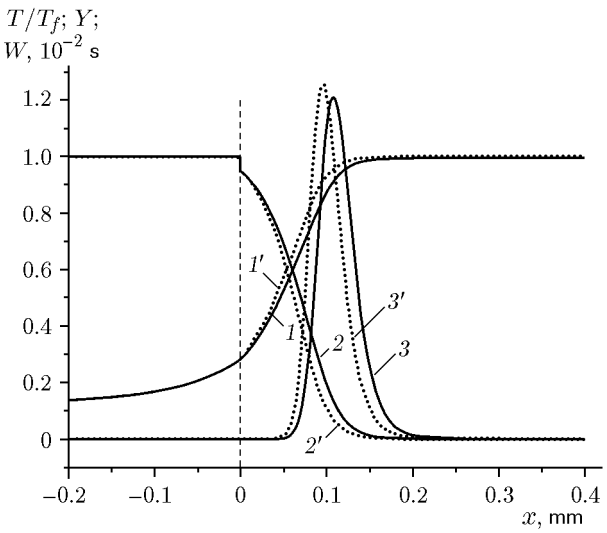

Fig. 3. Distributions of the temperature ratios T/T_f (curves *1* and *1′*), relative concentration Y (curves *2* and *2′*), and chemical reaction rate W (curves *3* and *3′*) with account for internal turbulence (*1–3*) and with no account for the internal turbulence (*1′–3′*); it is assumed that $Y = 1$ in the region $x < 0$, and T_f is the flame temperature.

Combustion becomes steady in time periods of the order of several values of the time of the thermal reaction of the solid phase $t_r = \varkappa_c(u')^{-2} \approx 1.2 \cdot 10^{-2}$ s, so the calculated time is $(8–10)t_r$. The solution of the model equations is sought for in the region from -1 to 2.3 mm. The width of the combustion zone δ_b is determined from the position of the maximum of the chemical reaction rate W.

3.1. Combustion in the Absence of Blowing and in the Presence of Internal Turbulence

Kolmogorov laws for locally isotropic turbulence superimpose restrictions on the nature and limits of changes in the kinetic energy e_k and scale l_t. The faster the energy e_k dissolves, the larger l_t becomes, but the coefficient of turbulent diffusion D_t decreases. Large values of a_1 accelerate the conversion of kinetic energy of turbulence into thermal energy, and the region of gas with turbulent motion concentrates near the gasification surface. Figure 2 shows the spatial distributions of the dimensionless scale l_t/d_b and transfer coefficient $D_t/\varkappa_0$ for $a_1 = 10^{-8}$ and 10^{-7}. In this figure and in Fig. 3, the origin of the x coordinate is the gasification surface.

The data from Fig. 2 make it possible to estimate the influence of a_1 on the nature of decay of internal turbulence, which plays an important role in the combustion of solid propellants. The combustion of a standard N powder is simulated below. It is assumed that the combustion zone has internal turbulence with parameters $a_1 = 10^{-10}$ and $b_1 = 10$, but there is no motion of the gaseous products of combustion along the gasification surface ($w_\infty = 0$). Equations (9) are not considered. The small value of a_1 is taken for simulating the weak decay of turbulence within the width limits of the combustion zone. The burning rate of the N powder is calculated using the following constants [44]: $u_* = 8.46$ m/s, $E_c = 7.98 \cdot 10^4$ J/mol, the temperature on the gasification surface in the case of steady combustion $T_s = T_{s0} = 658$ K, and burning rate $u_0 = 5.732$ mm/s at $p = 50$ atm.

The following parameters for the N powder are recommended additionally [10, 44]: $\rho_c = 1600$ Kg/m^3, $c_c = c_p = 1465$ J/(kg·K), $\lambda_c = 1.0$ J/(m·K·s), thermal effect of the reaction in the solid phase $Q_s = 2.53 \cdot 10^5$ J/kg and in the gaseous phase $Q = 2.73 \cdot 10^6$ J/kg, $R_g = 489$ J/(kg·K), $\langle d_b \rangle = 0.87 \cdot 10^{-7}$ m, $\sigma_s = 10^{-2}$ N/m, $D_0 = 1.1 \cdot 10^{-4}$ m^2/s, $\lambda_0 = 0.15$ J/(m·K·s), and $\nu_0 = 1.1 \cdot 10^{-4}$ m^2/s. These gas parameter values yield the value of the Lewis number Le = 0.75. Chemical reaction rate in the gaseous phase: $k_0 = 1.018 \cdot 10^{10}$ s^{-1}, and $E = 1.86 \cdot 10^5$ J/mol.

The main purpose of this study is to simulate the combustion of the N powder in the experiments [3], where the results for the erosion factor are presented in the form of a relationship with the Vilyunov number Vi and the interval Vi = 1–10 at $p = 50$ atm corresponds to changes in the velocity in the range $w_\infty = 12–140$ m/s.

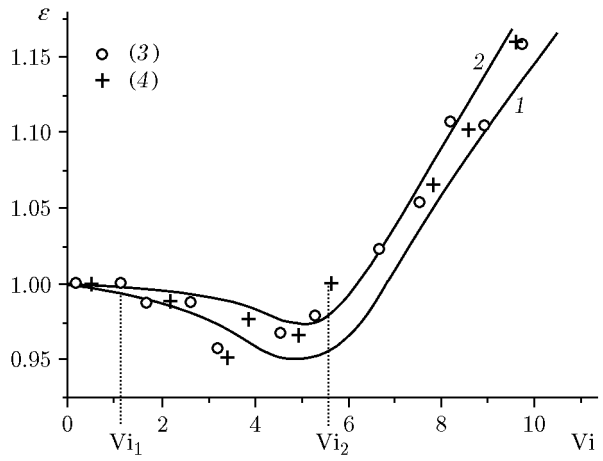

Fig. 4. Theoretical (curves *1* and *2*) and experimental (points *3* and *4*) [3] dependences of the erosion factor on the Vilyunov number for $p = 50$ (*1* and *3*) and 80 atm (*2* and *4*).

This circumstance superimposes restrictions on possible values of the molar mass of gas M_m and coefficients D_0 and ν_0 with chosen values of other parameters of the N powder.

Figure 3 shows the distributions of temperature, concentration, and chemical reaction rates in the absence and presence of internal turbulence, and they correspond to a burning rate $u_0 = 5.733$ mm/s. The flame temperature is $T_f = 2327$ K at $T_0 = 298$ K with account for internal turbulence and $T_f = 2334$ K with no account for it. It should be clarified that the flame temperature is understood as the temperature of the combustion products near the chemical reaction zone. The weak decay of turbulence and the limited abilities of the computational equipment prevent from calculations with large spatial scales. Therefore, a decrease in $T_f = 2327$ K is an apparent effect.

The thickness of the chemical reaction zone in the absence of internal turbulence equals $\delta_b \approx 0.1$ mm, the "inclusion" of turbulence increases the combustion zone up to $\delta_b \approx 0.12$ mm. Thus, the internal turbulence moves the flame away in the gaseous phase from the gasification surface.

3.2. Combustion with $w_\infty \neq 0$

Simulation in the presence of blowing is carried out for pressures $p = 50$ and 80 atm, the same as in the experiments [3] with the N powder on the study of erosive effects. The coefficient of hydrodynamic resistance is $\zeta = 0.03$, and the Prandtl number is $\mathrm{Pr} = 0.75$. Figure 4 shows calculation results for the erosion factor $\varepsilon(\mathrm{Vi})$, where the Vilyunov number Vi changes from 0 to 10.75. Accordingly, the interval of changes in the blowing velocity w_∞ is determined in the limits 0–130 m/s. In [3], it is noted that there are two threshold numbers Vi_1 and Vi_2, where Vi_1 characterizes the formation of a negative erosive effect, and Vi_2 is related to the recovery of the erosion factor up to a value $\varepsilon = 1$. In simulation, the number Vi_1 is not detected, and the burning rate smoothly decreases as Vi becomes larger.

The results for a pressure $p = 50$ atm are considered as follows. According to the experimental data [3], the erosion factor at $\mathrm{Vi} = \mathrm{Vi}_* \approx 3.7$ takes a minimal value $\varepsilon = \varepsilon_{\min} \approx 0.95$. It is theoretically obtained that $\mathrm{Vi}_* \approx 4.9$ (see Fig. 4). On the region $\mathrm{Vi} < \mathrm{Vi}_*$, the generation of turbulent mechanical energy and its return from the gasification zone into the flame zone play an important role, while the heat flux from the flame zone to the gasification surface remains the same. The negative energy balance arising from the turbulence reduces the erosion factor. The whole combustion zone is located inside the viscous sublayer of the outer turbulent boundary layer. The threshold number $\mathrm{Vi}_* \approx 4.9$ corresponds to the velocity $w_\infty \approx 60$ m/s. The thickness of the viscous sublayer for $\mathrm{Vi} = \mathrm{Vi}_*$ is $\delta_g = 0.257$ mm, and the thickness of the combustion zone is $\delta_b = 0.115$ mm, i.e., the Bulgakov–Lipanov threshold number is $\Theta_* \approx 0.45$. The parameter δ_g is determined from the spot where turbulent viscosity becomes equal to the molecular viscosity of gas. The thickness of the combustion zone δ_b is considered to be the distance from the gasification surface to the point where the chemical reaction rate is maximal. The pressure rise reduces the threshold values of Vi_* and Θ_*, and the negative erosive effect weakens along with them. This agrees with the experimental observations [6] if the mechanism of formation of the negative effect is assumed to be the same for all types of propellants. In the region $\mathrm{Vi} > \mathrm{Vi}_*$ (or $\Theta > \Theta_*$), the flame in the gaseous phase becomes turbulent, which strongly increases the heat flux from the flame zone to the gasification surface. The value of this heat flux exceeds the mechanical energy of turbulent motion, returned to the flame zone. Therefore, the erosion factor in this region is larger.

The gas temperature behind the chemical reaction zone monotonously decreases from 2327 to 2236 K with increasing blowing velocity w_∞ from 0 to 130 m/s. However, this does not mean that the flame temperature drops, and the simulation region small in space prevents from fully accounting for the energy dissipation of the turbulent motion of gas.

The experiments [3] reveal the universal dependence $\varepsilon(\mathrm{Vi})$: the erosion factor turns out to be the same at $p = 50$ and 80 atm. The comparison of theoretical results (see Fig. 4), obtained at $p = 50$ and 80 atm, does not reveal total universality. However, it can be seen in

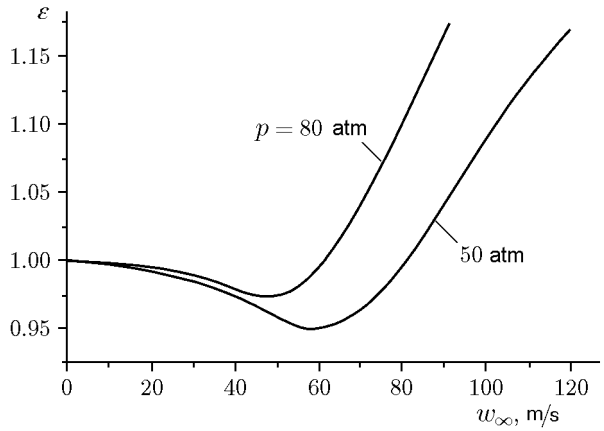

Fig. 5. Erosion factor versus the blowing velocity at $T_0 = 298$ K and different pressures.

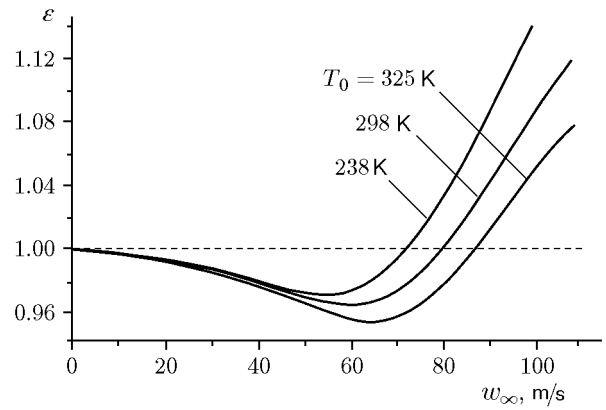

Fig. 6. Erosion factor versus the blowing velocity at $p = 50$ atm and different initial temperatures.

the comparison of $\varepsilon(w_\infty)$ in Fig. 5 and $\varepsilon(\mathrm{Vi})$ in Fig. 4 for the given pressures that the corresponding curves become closer in Fig. 4, i.e., Vi is sufficiently universal.

For the N powder, the negative erosive effect vanishes at $T_0 = 238$ K, and the minimal value is $\varepsilon_{\min} = 0.8$ at $T_0 = 325$ K [4]. The simulation shows a decrease in $\varepsilon_{\min}$ with reducing T_0 (Fig. 6), i.e., the theoretical results agree only qualitatively with the experimental data [4], where the dependence $\varepsilon_{\min}(T_0)$ is stronger than in Fig. 6. The minimal values of ε in this figure are as follows: $\varepsilon_{\min}(238\ \mathrm{K}) = 0.966$, $\varepsilon_{\min}(298\ \mathrm{K}) = 0.953$, and $\varepsilon_{\min}(325\ \mathrm{K}) = 0.95$.

The discovered difference between theoretical and experimental data can be explained the simplified nature of the combustion model, especially the rough representation of chemical reactions in the condensed phase of the propellant as there is a strong dependence of $\varepsilon_{\min}(T_0)$ on the activation energy E_c.

In previous studies [7–10], the manifestation of the Vilyunov–Dvoryashin effect is explained by the fact that some inner energy of gaseous products of combustion converts into their kinetic energy of motion with the velocity w. This energy conversion is accounted for by a complex as a source function

$$\frac{\rho}{2}\left(\frac{\partial w^2}{\partial t} + v\frac{\partial w^2}{\partial x}\right)$$

in the expression for $W_{g,s}$. In the tests [3, 4], this complex does not play a significant role, but its influence becomes significant in other experiments [5, 6], where the Vilyunov–Dvoryashin effect is manifested with $w_\infty \geqslant 150$ m/s.

CONCLUSIONS

The main results of the analysis of the presented combustion model and those obtained previously in [6, 17–19, 21, 34, 36] come down to the following.

1. Small-scale turbulence is formed with a large probability practically for all solid propellants near the gasification zone, and this turbulence differs in its intensity for various propellants.

2. The Vilyunov–Dvoryashin effect manifests as a result of conversion of some inner energy of gas or vapor–liquid phase into the mechanical energy of motion. If this transition occurs near the gasification zone, then part of the heat flux returns into the gaseous phase in the form of mechanical energy, and this "mirror effect" manifests as a thermal insulation.

3. The manifestation of the Vilyunov–Dvoryashin effect is almost improbable at high pressures and initial temperatures.

4. The possibility of the manifestation of the Vilyunov–Dvoryashin effect is high for propellants with low burning rates with a noticeable layer of liquid or vapor–liquid phase in the gasification zone.

REFERENCES

1. O. I. Leipunskii, *Physical Fundamentals of Internal Ballistics of Rocket Projectiles* (Semenov Inst. of Chem. Phys., Russian Acad. of Sci., Moscow, 1945) [in Russian].
2. K. O. Sabdenov, "On the Threshold Nature of Erosive Burning," Fiz. Goreniya Vzryva **44** (3), 127–132 (2008) [Combust., Expl., Shock Waves **44** (3), 300–309 (2008)].
3. V. N. Vilyunov and A. A. Dvoryashin "An Experimental Investigation of the Erosive Burning Effect," Fiz. Goreniya Vzryva **7** (1), 45–51 (1971) [Combust., Expl., Shock Waves **7** (1), 38–42 (1971)].

4. V. N. Vilyunov and A. A. Dvoryashin "Effect of the Initial Temperature of a Condensed Substance on the Value of the Negative Erosion," Fiz. Goreniya Vzryva **9** (4), 602 (1973) [Combust., Expl., Shock Waves **9** (4), 521–522 (1973)].
5. *Richard Nakka's Experimental Rocketry Web Site*, http://www.nakka-rocketry.net/burnrate. html.
6. N. Kubota, *Propellants and Explosives: Thermochemical Aspects of Combustion* (Wiley-VCH Verlag GmbH, Wainheim, 2007).
7. K. O. Sabdenov and M. Erzada, "Mechanism of the Negative Erosion Effect," Fiz. Goreniya Vzryva **49** (3), 22–33 (2013) [Combust., Expl., Shock Waves **49** (3), 273–282 (2013)].
8. K. O. Sabdenov and M. Erzada, "Mechanism of the Negative Erosion Effect," Fiz. Goreniya Vzryva **49** (6), 76–86 (2013) [Combust., Expl., Shock Waves **49** (6), 690–699 (2013)].
9. K. O. Sabdenov and M. Erzada, "Negative Erosion Effect and the Emergence of Unstable Combustion. 1. Analysis of the Models," Fiz. Goreniya Vzryva **52** (1), 76–83 (2016) [Combust., Expl., Shock Waves **52** (1), 67–73 (2016)].
10. authK. O. Sabdenov and M. Erzada, "Negative Erosion Effect and the Emergence of Unstable Combustion. 2. Numerical Simulation," Fiz. Goreniya Vzryva **52** (2), 76–87 (2016) [Combust., Expl., Shock Waves **52** (2), 193–202 (2016)].
11. V. A. Arkhipov, D. A. Zimin, E. A. Kozlov, and N. S. Tret'yakov, "Experimental Study of Erosive Burning of Solid Propellants," Khim. Fiz. **16** (9), 101–106 (1997).
12. V. A. Arkhipov and D. A. Zimin, "Erosive Burning of a Solid Propellant in a Supersonic Flow," Fiz. Goreniya Vzryva **34** (1), 61–64 (1998) [Combust., Expl., Shock Waves **34** (1), 55–57 (1998)].
13. S. Krishnan and K. K. Rajesh, "Erosive Burning Rate Studies of Composite Propellants Under High Cross Flow Velocities," AIAA-98-3384; http://arc.aiaa.org; DOI:10.2514/6.1998-3384.
14. G. I. Barenblatt, *Scaling, Self-Similarity, and Intermediate Asymptotics* (Gidrometeoizdat, Leningrad, 1982; Cambridge Univ. Press, Cambridge, 1996).
15. Y. M. Timnat, *Advanced Chemical Rocket Propulsion* (Academic Press, London, 1987).
16. L. K. Gusachenko and V. E. Zarko "Combustion Models for Energetic Materials with Completely Gaseous Reaction Products," Fiz. Goreniya Vzryva **41** (1), 24–40 (2005) [Combust., Expl., Shock Waves **41** (1), 20–34 (2005)].
17. V. K. Bulgakov and A. M. Lipanov, "Combustion of Condensed Material with Blowing," Fiz. Goreniya Vzryva **19** (3), 32–41 (1983) [Combust., Expl., Shock Waves **19** (3), 279–287 (1983)].
18. V. K. Bulgakov and A. M. Lipanov "Model of the Combustion of Solid Fuel with Blow-Off, Taking Account of the Interaction of Turbulence with the Chemical Reaction," Fiz. Goreniya Vzryva **20** (5), 68–74 (1984) [Combust., Expl., Shock Waves **20** (5), 538–542 (1984)].
19. V. K. Bulgakov, A. M. Lipanov, and A. Sh. Kamaletdinov, "Numerical Studies of the Erosional Combustion of Condensed Matter," Fiz. Goreniya Vzryva **22** (6), 83–88 (1986) [Combust., Expl., Shock Waves **22** (6), 717–721 (1986)].
20. D. R. Greatrix, "Model for Prediction of Negative and Positive Erosive Burning," Canadian Aeronaut. Space J. **53** (1), 13–21 (2007).
21. L. K. Gusachenko and V. E. Zarko "Erosive Burning. Modeling Problems," Fiz. Goreniya Vzryva **43** (3), 47–58 (2007) [Combust., Expl., Shock Waves **43** (3), 286–296 (2007)].
22. A. H. G. Isfahani, Ju Zhang, and T. L. Jackson, "Erosive Burning of Homogeneous and Heterogeneous Solid Propellants," in *45th AIAA/ASME/SAE/ASEE Joint Propulsion Conf. and Exhibit, Denver, August 2–5, 2009*; https://doi.org/10.2514/6.2009-5498.
23. Ju Zhang and T. L. Jackson, "A Model for Erosive Burning of Homogeneous Propellants," Combust. Flame **157**, 397–407 (2010).
24. T. L. Jackson, "Issues Related to Heterogeneous Solid-Propellant Combustion," Prog. Propul. Phys., No. 2, 3–20 (2011).
25. V. D. Topalian, J. Zhang, T. L. Jackson, and A. H. G. Isfahani, "Numerical Study of Erosive Burning in Multidimensional Solid Propellant Modeling," J. Propul. Power. **27** (4), 811–821 (2011).
26. D. R. Greatrix, "Influence of Initial Propellant Temperature on Solid Rocket Internal Ballistics," J. Propul. Power. **30** (4), 869–875 (2014).
27. V. Ya. Zyryanov, V. M. Bolvanenko, O. G. Glotov, and Yu. M. Gurenko "Turbulent Model for the Combustion of a Solid Fuel Composite," Fiz. Goreniya Vzryva **24** (6), 17–26 (1988) [Combust., Expl., Shock Waves **24** (6), 652–660 (1988)].
28. G. H. Markstein, *Nonsteady Flame Propagation* (Pergamon Press, 1964).
29. H. Schlichting, *Boundary Layer Theory* (Pergamon Press, 1955).
30. A. M. Klimov, "Flame Propagation in Strong Turbulence," Dokl. Akad. Nauk SSSR **221** (1), 56–59 (1975).
31. V. R. Kuznetsov and V. A. Sabel'nikov, *Turbulence and Combustion* (Nauka, Moscow, 1986) [in Russian].
32. K. O. Sabdenov, "Generation of Hydrodynamic Instability in the Gasification Region of Propellant," Fiz. Goreniya Vzryva **52** (6), 70–82 (2016) [Combust., Expl., Shock Waves **52** (6), 683–693 (2016)].

33. L. D. Landau, "On the Theory of Slow Combustion," in *Collected Papers of L.D. Landau* (Pergamon, 1965).
34. K. O. Sabdenov and M. Erzada, "Determination of the Transfer Coefficients of Natural Turbulence Occurring near the Solid-Propellant Gasification Zone. II. Hydrodynamic Instability in the Presence of Cross-Flow," Fiz. Goreniya Vzryva **53** (6), 26–37 (2017) [Combust., Expl., Shock Waves **53** (6), 641–651 (2017)].
35. K. O. Sabdenov and M. Erzada, "Anomalous Effect of Turbulence on the Burning Rate of Solid High-Energy Materials," Khim. Fiz. **37** (10), 51–59 (2018).
36. K. O. Sabdenov and M. Erzada, "Determination of the Transfer Coefficient of Natural Turbulence Occurring near the Solid-Propellant Gasification Zone. I. Two-Phase Model of the Gasification Zone," Fiz. Goreniya Vzryva **53** (5), 70–82 (2017) [Combust., Expl., Shock Waves **53** (5), 554–564 (2017)].
37. A. S. Monin and A. M. Yaglom, *Statistical Fluid Mechanics: Mechanics of Turbulence* (Massachusetts Inst. of Technology, Cambridge, 1975), Vol. 2.
38. L. D. Landau and E. M. Lifshitz, *Course of Theoretical Physics*, Vol. 6: *Fluid Mechanics* (Nauka, Moscow, 1986; Pergamon Press, 1959).
39. *Handbook of Turbulence: Fundamentals and Applications* Ed. by W. Frost and T. H. Moulden (Plenum Press, New York–London, 1977).
40. F. A. Williams, *Combustion Theory* (Addison-Wesley, Reading, 1964).
41. M. R. Denison and E. A. Baum, "A Simplified Model of Unstable Burning in Solid Propellants," ARS J. **31** 1112–1122 (1961).
42. K. O. Sabdenov and M. Erzada, "The Equation for Prandtls Mixing Length," Frontiers Aerosp. Eng. **3** (2), 50–55 (2014).
43. N. N. Kalitkin, *Numerical Methods* (Nauka, Moscow, 1978) [in Russian].
44. V. K. Bulgakov and A. M. Lipanov, "Combustion of Condensed Material with Blowing," Fiz. Goreniya Vzryva **19** (3), 32–41 (1983) [Combust., Expl., Shock Waves **19** (3), 279–287 (1983)].